FEBS Letters 581 (2007) 4778–4782

Peptide binding proclivities of calcium loaded calbindin-D28k

David R. Kordys[a], Benjamin G. Bobay[a], Richele J. Thompson[a], Ronald A. Venters[b], John Cavanagh[a,*]

[a] Department of Molecular and Structural Biochemistry, North Carolina State University, Raleigh, NC 27695, USA
[b] Duke University NMR Center, Durham, NC 27710, USA

Received 23 July 2007; accepted 3 September 2007

Available online 11 September 2007

Edited by Christian Griesinger

Abstract **Calbindin-D28k is known to function as a calcium-buffering protein in the cell. Moreover, recent evidence shows that it also plays a role as a sensor. Using circular dichroism and NMR, we show that calbindin-D28k undergoes significant conformational changes upon binding calcium, whereas only minor changes occur when binding target peptides in its Ca^{2+}-loaded state. NMR experiments also identify residues that undergo chemical shift changes as a result of peptide binding. The subsequent use of computational protein–protein docking protocols produce a model describing the interaction interface between calbindin-D28k and its target peptides.**

Keywords: Calbindin-D28k; NMR; Chemical shift; Peptides; Modeling

1. Introduction

Calcium is ubiquitous throughout the body, mediating many diverse cellular processes. Calcium signaling pathways are widely distributed and participate in all basic cellular functions, playing a key role in homeostasis [1–3]. Calcium regulation and signaling is achieved through interaction with an assortment of proteins known as calcium binding proteins (CaBPs). CaBPs have traditionally been distinguished by the role they play in the cell, as either calcium buffers (buffering and transport) or as calcium sensors (interactions with target proteins) [4].

Calbindin-D28k (261 residues, ~30 kDa) is a member of the calmodulin superfamily of intracellular Ca^{2+}-binding proteins [3]. It plays roles in protecting against excitotoxic cell death in hippocampal neurons, and in transcellular Ca^{2+} movement in intestinal absorptive cells and kidney distal tubules [5–7]. Calbindin-D28k also controls insulin release in pancreatic islet cells and co-localizes and interacts with the plasma membrane Ca^{2+} pump in the nervous system [6,8]. Early studies suggested that calbindin-D28k functioned solely as a calcium buffer [9]. However, it has now been established that it also exhibits calcium sensor properties [10–15]. Calbindin-D28k undergoes a structural transition from an ordered apo-conformation, through a disordered partially Ca^{2+}-loaded state, to a highly structured fully Ca^{2+}-loaded state [16]. Additionally, it has been shown that Ca^{2+}-loaded calbindin-D28k directly interacts with at least three target proteins, Ran-binding protein M (RanBPM), *myo*-inositol monophosphatase (IMPase), and caspase-3/procaspase-3 [10,11,13]. These observations suggest that it performs crucial functions as a sensor protein. RanBPM is a protein that regulates many functions, including the activity of GTP-bound Ran and microtubule assembly in cells [10]. IMPase is a key enzyme in the phosphatidylinositol second-messenger pathway. Calbindin-D28k also modulates apoptosis by binding caspase-3 and altering its activity in osteoblasts that mineralize bone [12,13,15]. There is an extra interest in calbindin-D28K/(pro)caspase-3 interactions in the onset of neurodegenerative diseases, where calbindin-D28k acts as a neuroprotector [17,18]. Caspases exist as inactive zymogens (procaspases) and become activated by proteolysis. In the case of caspase-3, the pro-domain is processed and cleaved to optimize active site positioning. If the processing and cleavage of the pro-domain is hampered, caspase-3 activity is affected [19].

Consequently, elucidating calbindin-D28k's sensor characteristics and identifying target peptide binding surfaces may assist in the development of new therapeutic approaches for the treatment of several disorders. Initial studies showed that homologous peptide sequences from RanBPM, IMPase and the pro-domain of procaspase-3 bound to Ca^{2+}-loaded calbindin-D28k. These peptide sequences are: LASIKNR (RanBPM), ISSIKEKYPSHS (IMPase), and SKSIKNLEP (procaspase-3) [20].

Here, we used circular dichroism (CD) and NMR chemical shift perturbations (CSP) to analyze the complexes between these three peptides and calbindin-D28k. CD experiments revealed that no major structural changes occurred upon target peptide binding and CSP studies showed that the protein/peptide interactions were specific. CSP identified calbindin-D28k residues involved in peptide binding. Residues defined as 'active' through CSP were used as restraints in the molecular protein–protein docking program HADDOCK to model the protein/peptide interactions between calbindin-D28k and RanBPM, IMPase, and caspase-3. This docking analysis revealed a contiguous target binding surface in the region of EF-hand 2.

2. Materials and methods

2.1. Sample preparation

Cloning, expression, and purification protocols for *Rattus norvegicus* calbindin-D28k have been described [16]. Peptides used in the NMR titrations and CD experiments are as follows: RanBPM (LASIKNR),

*Corresponding author. Fax: +1 919 515 2057.
E-mail address: john_cavanagh@ncsu.edu (J. Cavanagh).

0014-5793/$32.00
doi:10.1016/j.febslet.2007.09.004

IMPase (ISSIKEKYPSHS), procaspase-3 (SKSIKNLEP) (Sigma Genosys), and a negative control C28R2 (LRRGQILWFRGLNRIQTQIRVVKAFRSS) (AnaSpec).

2.2. Circular dichroism

CD spectra were measured using a PiStar Kinetic Circular Dichroism Spectrometer using a 1 cm (near-UV) Hellma cuvette (Hellma Corp.). Measurements were corrected for background and peptide signal. Buffer conditions were subtracted under the same experimental conditions. Spectra were recorded in 10 mM Tris pH 6.25, and 1 mM $CaCl_2$ for Ca^{2+}-loaded calbindin-D28k samples and 10 mM Tris pH 6.25 and 1 mM EDTA for apo-calbindin-D28k samples. Protein/peptide complexes were combined at 1:1, 1:4, 1:8, 1:12, 1:16 ratios and calbindin-D28k concentration was held at 60 μM. Complexes were incubated overnight at room temperature prior to CD analysis. Spectra were recorded five times and averaged at 25 ± 1.0 °C from 250 to 320 nm.

2.3. NMR peptide titrations

NMR samples contained ~0.5 mM Ca^{2+}-loaded calbindin-D28k (pH 6.2, 10 mM Tris, 1 mM DTT, 0.02% (w/v) NaN_3, 3 mM $CaCl_2$, and 10% (v/v) D_2O). Peptides from RanBPM, IMPase, procaspase-3, and the negative control C28R2 were titrated into samples in increments that provided the following peptide/protein molar ratios: 0:1, 1:1, 2:1, 4:1, 8:1, and 16:1. At each titration point, a ^1H–^{15}N HSQC-TROSY experiment was collected at 25 °C on a Varian Inova 600 MHz spectrometer using a $^1H/^{13}C/^{15}N$ triple-resonance Z-gradient probe. Data were processed using NMRPipe and analyzed using NMRView [21,22].

2.4. High ambiguity driven protein–protein docking (HADDOCK)

The coordinate file for Ca^{2+}-loaded calbindin-D28k, was obtained from the RCSB Protein Data Bank (PDB, 2G9B) [23]. The coordinate files for peptides RanBPM, IMPase, and procaspase-3, were generated using PYMOL (http://pymol.sourceforge.net). Protein residues located in the predicted interaction interface were defined as 'active'. These assignments were based on CSP data generated via NMR protein/peptide titrations. All active residues exhibit a relative solvent accessibility >30% as delineated by the program NACCESS [24]. The following residues were defined as active: S4, H5, Q7, I11, T12, E18, E57, I73, G74, I75, A79, V81, E86, L89, R93, Q96, S99, C100, L153, and L180. For each peptide all residues were classified active. No residues in the protein were defined as being 'passive' (residues with solvent accessibility >30% surrounding active residues identified from CSP data). Default HADDOCK parameters were used in the docking procedure. Final structures were grouped using a minimum cluster size of 40 and an RMSD <3 Å using the program ProFit (http://www.bioinf.org.uk/software/profit/). The resulting clusters were analyzed and ranked according to their average interaction energies.

3. Results

3.1. Circular dichroism

Calbindin-D28k has been shown by NMR to undergo a large conformational change upon sequential calcium binding [16]. CD was used to investigate the structural transitions that

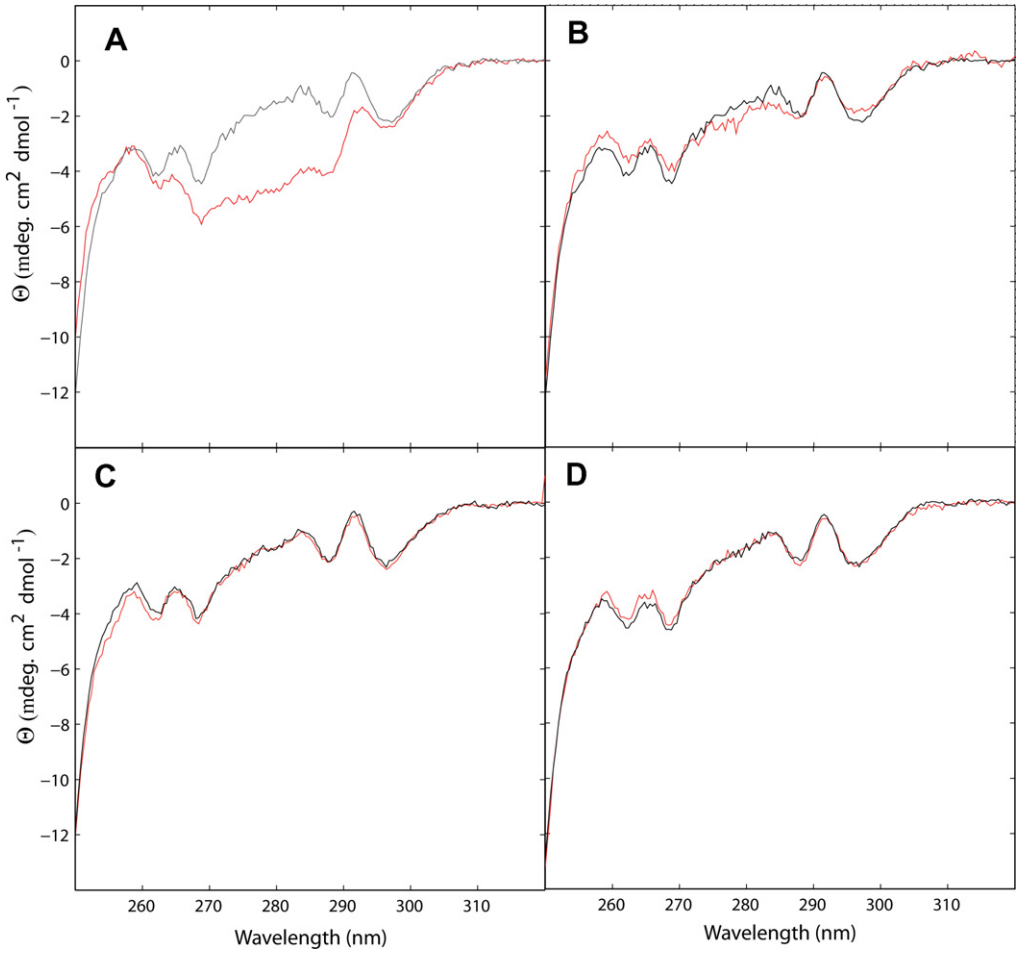

Fig. 1. Near-UV circular dichroism spectra. (A) comparison of apo calbindin-D28k (red) with Ca^{2+}-loaded calbindin-D28k showing a large conformational change. Spectra of calbindin-D28k alone (black) and with 1:16 ratio of calbindin-D28k:peptide (red) using (B) IMPase (C) RanBPM, and (D) procaspase-3. No gross conformational changes occur upon peptide binding.

occur upon peptide binding. The near-UV CD spectra of Ca^{2+}-loaded and apo-calbindin-D28k are shown in Fig. 1A. In agreement with previous studies, a major conformational change is seen, with the main differences in the tryptophan region (~280 nm) indicating a L_a-band transition [25].

The near-UV CD spectrum of Ca^{2+}-loaded calbindin-D28k was monitored during serial titrations with the synthesized peptides up to a 16:1 peptide:protein molar ratio, in order to investigate whether changes occur upon binding. No major conformational changes were observed as calbindin-D28k bound the peptides (Fig. 1B–D). Subtle differences were identified (in the region of the spectrum commonly attributed to phenylalanine absorption, 260 nm), indicative of ligand binding and slight alterations of the tertiary structure [26].

3.2. NMR peptide titrations

The RanBPM, IMPase, and procaspase-3 peptides were titrated into Ca^{2+}-loaded calbindin-D28k. Chemical shift changes and line broadening were monitored via ^{1}H–^{15}N HSQC-TROSY experiments (Fig. 2). These perturbations were quantified by calculating the cumulative chemical shift ($\Delta\delta$ppm) where:

$$\Delta\delta\text{ppm} = [\Delta\delta(^{1}H)^{2} + 0.1^{*}\Delta\delta(^{15}N)^{2}]^{1/2} \quad (1)$$

$\Delta\delta(^{1}H)$ is the proton chemical shift change and $\Delta\delta(^{15}N)$ is the nitrogen chemical shift change. Upon addition of the individual peptides some residues undergo little to no chemical shift, such as R249, E210, and L54 (<0.05 ppm). Other residues experience larger changes, e.g. L43 and E86 (>0.20 ppm) (Fig. 2A–C). In each titration, calbindin-D28k residues show similar overall chemical shift changes, although the extent of shift and direction varies slightly from peptide to peptide. This indicates a similar binding response for all ligands studied.

The regions of calbindin-D28k showing notable chemical shift changes were: A2–T12, E18, E57, K72–F117, L130–N135, L153–D155, K161–I184, E220–L226, and I255-N261. Two classes of chemical shifts are apparent in this group. The first class, A2–T12, E18, E57, L130–N135, L153–D155, K161–I184, E220–L226, and I255–N261, includes residues which undergo large chemical shift changes ($\Delta\delta$ppm > 0.20 ppm). The second class, K72–F117 involves a subset of residues that experience chemical shift changes and/or line broadening, indicative of conformational exchange. In order to determine if the interaction with the target peptides was specific, a negative control peptide was designed (C28R2). This peptide corresponds to the C-terminal tail of PMCA, a known calmodulin target [27]. Titration of this peptide into Ca^{2+}-loaded calbindin-D28k resulted in no chemical shift changes (Fig. 2D). This indicates that the binding observed for the peptides of interest is specific and not a result of non-specific interactions.

3.3. HADDOCK modeling

Areas within calbindin-D28k that undergo significant chemical shift perturbations with chemical shifts on average >0.20 ppm upon peptide binding were used as a basis for determining active interface residues in the calbindin-D28k:peptide complexes. For each modeling procedure, a series of ambiguous interaction restraints were generated based on CSP data and used in conjunction with the coordinate files for Ca^{2+}-loaded calbindin-D28k and the respective peptides. The docking procedure consists of three stages: rigid body energy minimization, semi-flexible refinement with simulated annealing, and explicit water refinement. The result of the docking protocol is 200 refined protein:peptide complexes, which were subsequently clustered as a function of their backbone RMSD

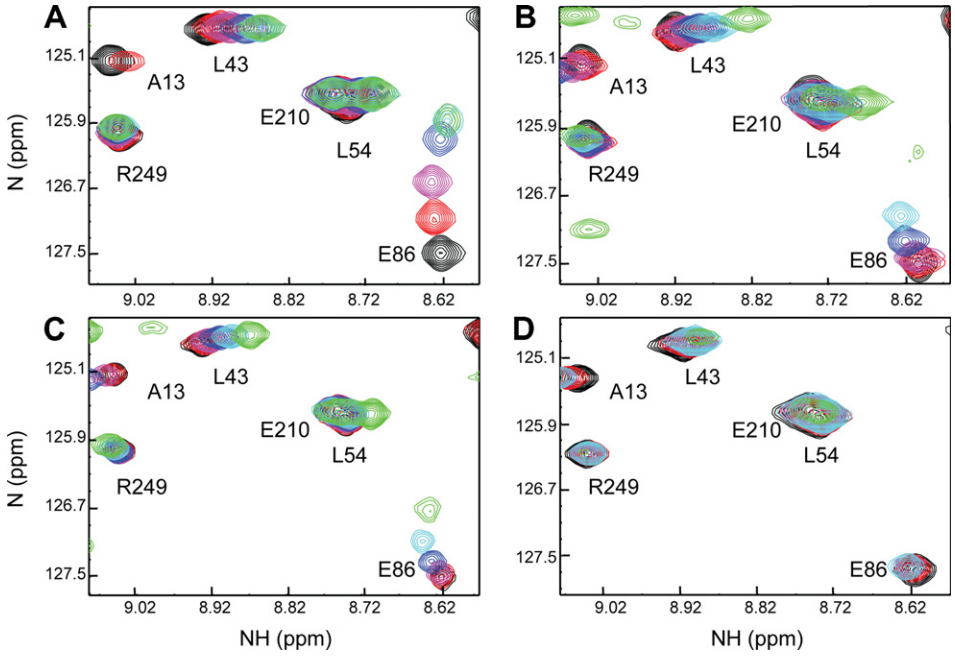

Fig. 2. Peptide titrations of calcium loaded calbindin-D28k. (A–D) Selected regions of ^{1}H–^{15}N HSQC-TROSY spectra of calbindin-D28k binding to target peptides from (A) RanBPM (B) IMPase (C) procaspase-3 and (D) C28R2 control. Spectra were collected at peptide:protein ratios of 0:1 (black), 1:1 (red), 2:1 (magenta), 4:1 (blue), 8:1 (cyan), and 16:1 (green).

from the lowest energy structure. Each modeling protocol resulted in two clusters, arising from two possible linear orientations of the peptide. For each peptide studied the lowest energy/best solution cluster maps to the same region of calbindin-D28k, consisting of α3/α4 of EF-hand 2 (EF-2), α8 of EF-4, and αA in the linker region between EF-2 and EF-3. The nature of the interaction is exemplified by the IMPase peptide–calbindin-D28k complex in Fig. 3A. The average total interaction energy for each model is -11812 ± 112 kcal/mol^{-1} (IMPase), -11512 ± 99 kcal/mol^{-1} (RanBPM), and -11643 ± 117 kcal/mol^{-1} (procaspase-3). These structures have an average buried surface energy of 1983 ± 90 Å^2, 1446 ± 63 Å^2, and 1666 ± 73 Å^2, respectively. Detailed structure statistics are given in Supplementary materials (Table 1). Analysis of the interaction interface from the 20 best structures taken from the lowest energy cluster identifies potential intermolecular hydrogen bonds for each complex. For example, seven potential hydrogen bonds were identified in the IMPase low energy cluster, consisting of Q7:S12, S8:S12, R47:S12, R93:E6, Q96:S3, V173:S3, and E175:I1 with respect to calbindin-D28k:IMPase (Fig. 3B). A full list of potential hydrogen bonds for all calbindin-D28k:peptide complexes is provided in Supplementary material (Table 2). Further analysis of the protein:peptide interface reveals two nearby aromatic residues: F92 and F61 (See Fig. 3B). Perturbation of these residues likely accounts for the phenylalanine absorption changes observed in the CD spectrum of the calbindin-D28k:peptide titrations.

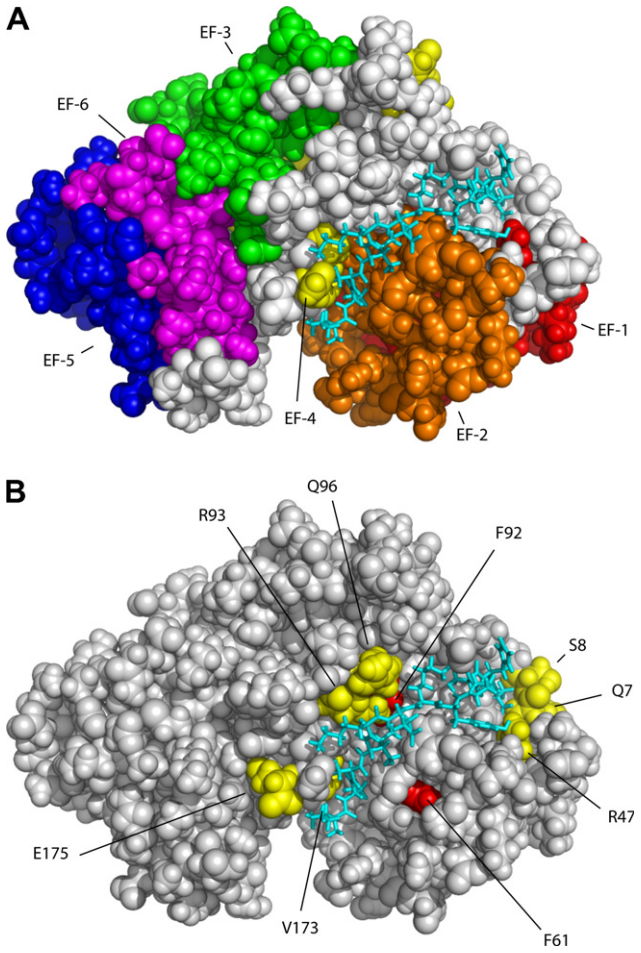

Fig. 3. HADDOCK modeling of IMPase peptide. (A) Model of Ca^{2+}-loaded calbindin-D28k bound to IMPase peptide (lowest energy model from cluster 2) displayed as a PyMOL surface plot. EF-hands from calbindin-D28k colored EF-1 (red) EF-2 (orange) EF-3 (green), EF-4 (yellow), EF-5 (blue), EF-6 (magenta). (B) Same surface plot with residues from calbindin-D28k involved in hydrogen bonding (Q7, S8, R47, Q96, R93, V173, and E175) colored yellow with F61 and F92 highlighted in red.

4. Discussion

Calcium binding proteins are key elements of cellular signaling and calcium homeostasis. Variations in the conformational response to calcium binding are indicators of the role of these proteins as either buffers or sensors. Calcium buffers typically exhibit little to no structural perturbations upon calcium binding, allowing for their high buffering capacity and structural stability. Conversely, calcium signaling proteins typically undergo large conformational changes in response to calcium, exposing a hydrophobic patch which allows for downstream protein/protein interactions. Earlier work in this laboratory demonstrated that apo-calbindin-D28k adopts an ordered conformation that changes significantly upon calcium loading. Here we report detailed information concerning the structural perturbations associated with the interaction between Ca^{2+}-loaded calbindin-D28k and peptides derived from three of its protein targets and use molecular modeling to describe a model for the interaction interface.

Elucidation of the high resolution structure of Ca^{2+}-loaded calbindin-D28k has allowed for a more thorough analysis of its interactions with peptides derived from RanBPM, IMPase, and procaspase-3. CD was used to monitor changes in tertiary conformation, as UV absorption/emission bands of aromatic amino acid side chains are visible in this spectrum. Only very minor changes in the conformation of Ca^{2+}-loaded calbindin-D28k are seen upon titration with peptides, in contrast to the large changes seen upon addition of calcium (Fig. 1). Peptide titration did result in perturbation of phenylalanine residue signal absorption, which typically has a strong component around 260 nm.

Protein/peptide NMR titrations were used to identify residues that are directly involved in and proximal to the binding interface. Because the chemical environment surrounding residues is affected by chemical bonding and molecular conformations, the CSP resulting from titration with the peptide can be used as a marker to identify residues that are actively involved in peptide binding. Similar chemical shift changes undergone by residues in the presence of peptides derived from RanBPM, IMPase, and procaspase-3 indicate that all three targets bind to the same site. Molecular modeling of these complexes identified the protein:peptide interaction site as α3/α4 of EF-hand 2 (EF-2), α8 of EF-4, and αA in the linker region between EF-2 and EF-3.

Particularly interesting is that the protein–peptide interaction is dominated by the EF2-αA region. EF2 does not bind Ca^{2+} and NMR H/N linewidths for residues in this region are ~15% broader than their counterparts in EF1. Also, the RMSD of the αA segment of calbindin-D28k (residues 82–100) is the highest in the protein (1.7 Å). These two pieces of information imply that the EF2-αA section of the protein shows conformational flexibility. Such flexibility may enable this single region to accommodate the multiple, different

binding partners known to interact with calbindin-D28k. Finally, since the EF2-αA region is not involved in calcium binding, it may be possible for calbindin-D28k to perform its buffering and signaling roles simultaneously.

Acknowledgements: This work was supported by Grants from the Kenan Institute for Engineering, Science and technology (J.C.) and the American Foundation for Aging Research (D.R.K.). The NCSU and Duke University NMR Centers were established with grants from the NIH, NSF, and the North Carolina Biotechnology Center.

Appendix A. Supplementary material

Supplementary data associated with this article can be found, in the online version, at doi:10.1016/j.febslet.2007.09.004.

References

[1] Berridge, M.J., Lipp, P. and Bootman, M.D. (2000) The versatility and universality of calcium signalling. Nat. Rev. Mol. Cell Biol. 1, 11–21.
[2] Bootman, M.D., Collins, T.J., Peppiatt, C.M., Prothero, L.S., MacKenzie, L., De Smet, P., Travers, M., Tovey, S.C., Seo, J.T., Berridge, M.J., Ciccolini, F. and Lipp, P. (2001) Calcium signalling – an overview. Semin. Cell Dev. Biol. 12, 3–10.
[3] Gross, M. and Kumar, R. (1990) Physiology and biochemistry of vitamin D-dependent calcium binding proteins. Am. J. Physiol. 259, F195–F209.
[4] Ikura, M. (1996) Calcium binding and conformational response in EF-hand proteins. Trend Biochem. Sci. 21, 14–17.
[5] Pochet, R., Blachier, F., Gangji, V., Kielbaska, V., Duee, P.H. and Resibois, A. (1990) Calbindin-D28k in mammalian intestinal absorptive cells: immunohistochemical evidence. Biol. Cell. 70, 91–99.
[6] Borke, J.L., Caride, A., Verma, A.K., Penniston, J.T. and Kumar, R. (1989) Plasma membrane calcium pump and 28-kDa calcium binding protein in cells of rat kidney distal tubules. Am. J. Physiol. 257, F842–F849.
[7] Mattson, M.P., Rychlik, B., Chu, C. and Christakos, S. (1991) Evidence for calcium-reducing and excito-protective roles for the calcium-binding protein calbindin-D28k in cultured hippocampal neurons. Neuron 6, 41–51.
[8] Sooy, K., Schermerhorn, T., Noda, M., Surana, M., Rhoten, W.B., Meyer, M., Fleischer, N., Sharp, G.W. and Christakos, S. (1999) Calbindin-D(28k) controls [Ca^{2+}](i) and insulin release. Evidence obtained from calbindin-d(28k) knockout mice and beta cell lines. J. Biol. Chem. 274, 34343–34349.
[9] Roberts, W.M. (1994) Localization of calcium signals by a mobile calcium buffer in frog saccular hair cells. J. Neurosci. 14, 3246–3262.
[10] Lutz, W., Frank, E.M., Craig, T.A., Thompson, R., Venters, R.A., Kojetin, D., Cavanagh, J. and Kumar, R. (2003) Calbindin-D28K interacts with Ran-binding protein M: identification of interacting domains by NMR spectroscopy. Biochem. Biophys. Res. Commun. 303, 1186–1192.
[11] Berggard, T., Szczepankiewicz, O., Thulin, E. and Linse, S. (2002) Myo-inositol monophosphatase is an activated target of calbindin-D28k. J. Biol. Chem. 277, 41954–41959.
[12] Christakos, S. and Liu, Y. (2004) Biological actions and mechanism of action of calbindin in the process of apoptosis. J. Steroid Biochem. Mol. Biol. 89–90, 401–404.
[13] Bellido, T., Huening, M., Raval-Pandya, M., Manolagas, S.C. and Christakos, S. (2000) Calbindin-D28k is expressed in osteoblastic cells and suppresses their apoptosis by inhibiting caspase-3 activity. J. Biol. Chem. 275, 26328–26332.
[14] Rabinovitch, A., Suarez-Pinzon, W.L., Sooy, K., Strynadka, K. and Christakos, S. (2001) Expression of calbindin-D(28k) in a pancreatic islet beta-cell line protects against cytokine-induced apoptosis and necrosis. Endocrinology 142, 3649–3655.
[15] Liu, Y., Porta, A., Peng, X., Gengaro, K., Cunningham, E.B., Li, H., Dominguez, L.A., Bellido, T. and Christakos, S. (2004) Prevention of glucocorticoid-induced apoptosis in osteocytes and osteoblasts by calbindin-D28k. J. Bone Miner. Res. 19, 479–490.
[16] Venters, R.A., Benson, L.M., Craig, T.A., Bagu, J., Paul, K.H., Kordys, D.R., Thompson, R., Naylor, S., Kumar, R. and Cavanagh, J. (2003) The effects of Ca^{2+} binding on the conformation of calbindin D(28k): a nuclear magnetic resonance and microelectrospray mass spectrometry study. Anal. Biochem. 317, 59–66.
[17] Cotman, C.W., Poon, W.W., Rissman, R.A. and Blurton-Jones, M. (2005) The role of caspase cleavage of tau in Alzheimer disease neuropathology. J. Neuropathol. Exp. Neurol. 64, 104–112.
[18] Wellington, C.L., Singaraja, R., Ellerby, L., Savill, J., Roy, S., Leavitt, B., Cattaneo, E., Hackam, A., Sharp, A., Thornberry, N., Nicholson, D.W., Bredesen, D.E. and Hayden, M.R. (2000) Inhibiting caspase cleavage of huntingtin reduces toxicity and aggregate formation in neuronal and nonneuronal cells. J. Biol. Chem. 275, 19831–19838.
[19] Donepudi, M. and Grutter, M.G. (2002) Structure and zymogen activation of caspases. Biophys. Chem. 101–102, 145–153.
[20] Kojetin, D.J., Venters, R.A., Kordys, D.R., Thompson, R.J., Kumar, R. and Cavanagh, J. (2006) Structure, binding interface and hydrophobic transitions of Ca^{2+}-loaded calbindin-D(28k). Nat. Struct. Mol. Biol. 13, 641–647.
[21] Delaglio, F., Grzesiek, S., Vuister, G.W., Zhu, G., Pfeifer, J. and Bax, A. (1995) NMRPipe: a multidimensional spectral processing system based on UNIX pipes. J. Biomol. NMR 6, 277–293.
[22] Johnson, B.A. (2004) Using NMRView to visualize and analyze the NMR spectra of macromolecules. Meth. Mol. Biol. 278, 313–352.
[23] Berman, H., Henrick, K. and Nakamura, H. (2003) Announcing the worldwide Protein Data Bank. Nat. Struct. Biol. 10, 980.
[24] Hubbard, S.J. and Thornton, J.M. (1993) Department of Biochemistry and Molecular Biology, University College London.
[25] Venyaminov, S.Y., Klimtchuk, E.S., Bajzer, Z. and Craig, T.A. (2004) Changes in structure and stability of calbindin-D(28k) upon calcium binding. Anal. Biochem. 334, 97–105.
[26] Greenfield, N.J. (2004) Circular dichroism analysis for protein–protein interactions. Meth. Mol. Biol. 261, 55–78.
[27] Filoteo, A.G., Enyedi, A. and Penniston, J.T. (1992) The lipid-binding peptide from the plasma membrane Ca^{2+} pump binds calmodulin, and the primary calmodulin-binding domain interacts with lipid. J. Biol. Chem. 267, 11800–11805.